



# Technical Note: Integrating an open source Monte Carlo code “MCsquare” for clinical use in intensity-modulated proton therapy

Wei Deng and James E. Younkin

*Department of Radiation Oncology, Mayo Clinic, Phoenix, AZ 85054, USA*

Kevin Souris

*Center for Molecular Imaging and Experimental Radiotherapy, Institut de Recherche Expérimentale et Clinique, Université catholique de Louvain, 1200, Brussels, Belgium*

Sheng Huang

*Department of Medical Physics, Memorial Sloan Kettering Cancer Center, New York, NY, USA*

Kurt Augustine, Mirek Fatyga, and Xiaoning Ding

*Department of Radiation Oncology, Mayo Clinic, Phoenix, AZ 85054, USA*

Marie Cohilis

*Center for Molecular Imaging and Experimental Radiotherapy, Institut de Recherche Expérimentale et Clinique, Université catholique de Louvain, 1200, Brussels, Belgium*

Martin Bues, Jie Shan, and Joshua Stoker

*Department of Radiation Oncology, Mayo Clinic, Phoenix, AZ 85054, USA*

Liyong Lin

*Emory Proton Therapy Center, Emory University, Atlanta, GA, USA*

Jiajian Shen<sup>a)</sup> and Wei Liu<sup>a)</sup>

*Department of Radiation Oncology, Mayo Clinic, Phoenix, AZ 85054, USA*

(Received 11 October 2019; revised 27 February 2020; accepted for publication 27 February 2020; published 13 April 2020)

**Purpose:** To commission an open source Monte Carlo (MC) dose engine, “MCsquare” for a synchrotron-based proton machine, integrate it into our in-house C++-based I/O user interface and our web-based software platform, expand its functionalities, and improve calculation efficiency for intensity-modulated proton therapy (IMPT).

**Methods:** We commissioned MCsquare using a double Gaussian beam model based on in-air lateral profiles, integrated depth dose of 97 beam energies, and measurements of various spread-out Bragg peaks (SOBPs). Then we integrated MCsquare into our C++-based dose calculation code and web-based second check platform “DOSeCHECK.” We validated the commissioned MCsquare based on 12 different patient geometries and compared the dose calculation with a well-benchmarked GPU-accelerated MC (gMC) dose engine. We further improved the MCsquare efficiency by employing the computed tomography (CT) resampling approach. We also expanded its functionality by adding a linear energy transfer (LET)-related model-dependent biological dose calculation.

**Results:** Differences between MCsquare calculations and SOBP measurements were <2.5% (<1.5% for ~85% of measurements) in water. The dose distributions calculated using MCsquare agreed well with the results calculated using gMC in patient geometries. The average 3D gamma analysis (2%/2 mm) passing rates comparing MCsquare and gMC calculations in the 12 patient geometries were  $98.0 \pm 1.0\%$ . The computation time to calculate one IMPT plan in patients’ geometries using an inexpensive CPU workstation (Intel Xeon E5-2680 2.50 GHz) was  $2.3 \pm 1.8$  min after the variable resolution technique was adopted. All calculations except for one craniospinal patient were finished within 3.5 min.

**Conclusions:** MCsquare was successfully commissioned for a synchrotron-based proton beam therapy delivery system and integrated into our web-based second check platform. After adopting CT resampling and implementing LET model-dependent biological dose calculation capabilities, MCsquare will be sufficiently efficient and powerful to achieve Monte Carlo-based and LET-guided robust optimization in IMPT, which will be done in the future studies. © 2020 American Association of Physicists in Medicine [https://doi.org/10.1002/mp.14125]

Key words: dose calculation, intensity-modulated proton therapy (IMPT), Mcsquare, Monte Carlo method, robust optimization

## 1. INTRODUCTION

Generally speaking, Monte Carlo (MC) simulations are more accurate than analytical dose calculation algorithms, but general purpose MC codes (e.g., Geant4,<sup>1</sup> MCNPX,<sup>2</sup> FLUKA,<sup>3,4</sup> and TOPAS<sup>5</sup>), although they are very accurate,<sup>1–5</sup> but relatively slow and very tedious for routine clinical use. On the other hand, analytical dose engines<sup>6–8</sup> for intensity-modulated proton therapy (IMPT), although they cannot handle heterogeneity as accurately as MC simulation in highly heterogeneity regions,<sup>9</sup> are still widely used in the commercial and many in-house treatment planning systems (TPSs) due to their fast calculation speed. Recently, some groups had developed several fast MC codes, for example, gMC,<sup>10</sup> gPMC,<sup>11</sup> FRED,<sup>12</sup> and MCsquare,<sup>13</sup> which are dedicated to proton dose calculation with simplified physics model and/or with the help of GPU acceleration to significantly reduce the simulation time with acceptable compromise of accuracy compared with general purpose MC codes. Some commercial TPSs with fast MC calculation capability have recently been released for routine clinical use (e.g., RayStation,<sup>14</sup> Eclipse<sup>15</sup>).<sup>16</sup>

With improvements in hardware and coding techniques, MC dose engines have become efficient enough for potential use as second check dose engines and for robust optimization.<sup>17–28</sup> However, for most institutions, development of a fast in-house MC code would be time consuming. An open source fast MC code like MCsquare (about 20–35 times faster<sup>13</sup> than Geant4) is an alternative to these options with several advantages: (a) it can introduce the supplemental MC capability to an existing in-house developed or commercial TPSs without developing new MC codes, (b) it is easy to add new features to the open-source code, such as MC-based robust optimization<sup>17,29</sup> and relative biological equivalent (RBE) model study based on patient outcome correlation, MC-based robustness evaluation,<sup>30</sup> and four-dimensional (4D) dose calculation (including interplay effects evaluation). Also, the material database is easily modifiable and expendable in MCsquare, and (c) several institutions<sup>13,31,32</sup> have successfully implemented MCsquare and different institutions can easily collaborate or share upgrades and perform cross-checks for accuracy.

Despite these advantages, integrating a fast MC code such as MCsquare into existing clinical software platforms is not straightforward. MCsquare was developed using the C programming language with “Cilk Plus” extension. Although MCsquare is an independent MC package, users have the option to use a third party software (e.g., “OpenREGGUI” platform based on MATLAB) to handle various pre- and postprocessing tasks including DICOM file conversion, structure density overwrite, and body volume cropping. This is a good approach for an independent package for general users. However, in order to integrate it into a specific routine clinical practice, streamline the user workflow, allow for the use from various platforms, and further improve the efficiency of the code by employing the message passing interface (MPI) capability for optimization, we needed several

additional modifications. On the other hand, as far as we know, MCsquare commissioning was only reported for the cyclotron system.<sup>13,31,32</sup> Due to the differences in the beam source phase space between cyclotron and synchrotron-based proton therapy systems (such as continuous vs discrete energies, narrow energy dispersion vs wide energy dispersion), it was not straightforward to commission the MCsquare package for a synchrotron-based proton therapy system and validate whether MCsquare with a Gaussian-based beam source model can accurately calculate the dose for a synchrotron-based proton therapy system, even if the particle transportation in the medium is the same.

In this paper, we report our approaches to (a) successfully commissioning open source MCsquare to a synchrotron-based proton system for the first time, (b) using MCsquare as a library and integrating it into our C++-based dose calculation code with MPI capability, web-based second check, and patient quality assurance software platform,<sup>33,34</sup> (c) significantly improving the simulation efficiency by introducing the computed tomography (CT) resampling approach, and (d) expanding its capability by adding a model-dependent biological dose calculation function. After these approaches, our new user interface became straightforward and could be executed from various terminals (e.g., desktop, laptop, tablet, or phone).

## 2. METHODS AND MATERIALS

### 2.A. Commissioning MCsquare

The proton system in our center provides 97 discrete beam energies (71.3–228.8 MeV) generated using a synchrotron accelerator.<sup>35</sup> In the Eclipse treatment planning system, three beam models (VAC, RS, and ERS) were commissioned for clinical use, which represent the treatment types: without range shifter (VAC), with 45 mm water equivalent thickness (WET) range shifter (RS) at regular position (42.5 cm from isocenter), and similar range shifter at extended position (30 cm from isocenter) (ERS). We commissioned MCsquare to get a single set of phase space parameters suitable for all three machines. In order to speed up the calculation we did not simulate the particle transport in the nozzle. Instead we derived the phase space using integrated depth dose (IDD) curves and in-air lateral profiles at five positions of proton beams distal to the nozzle (but before the range shifter). Hence, the phase space has a large emittance due to the scattering of the beamline components in the nozzle,<sup>36,37</sup> and we chose to use double Gaussian lateral profile to model the beam source more accurately.<sup>31,32</sup> The detailed methods, parameters, and formulas are described in the MCsquare user manual<sup>38</sup> and the validation of physics model of MCsquare is described in Souris *et al.*<sup>13</sup> For our synchrotron-based system we commissioned 97 discrete energies, rather than a selected number of energies as are typical for a cyclotron-based system.<sup>31</sup> In the paper, we focus on the details of the commissioning and fine-tuning process for our synchrotron-based proton machine.

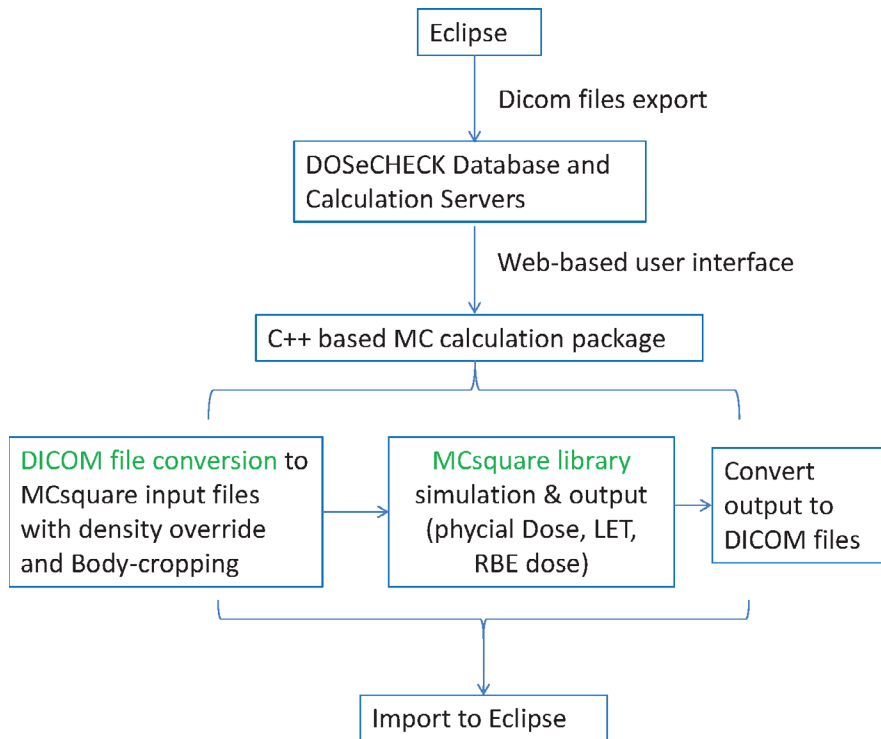


Fig. 1. Workflow of using MCsquare in the DOSeCHECK software platform. [Color figure can be viewed at wileyonlinelibrary.com]

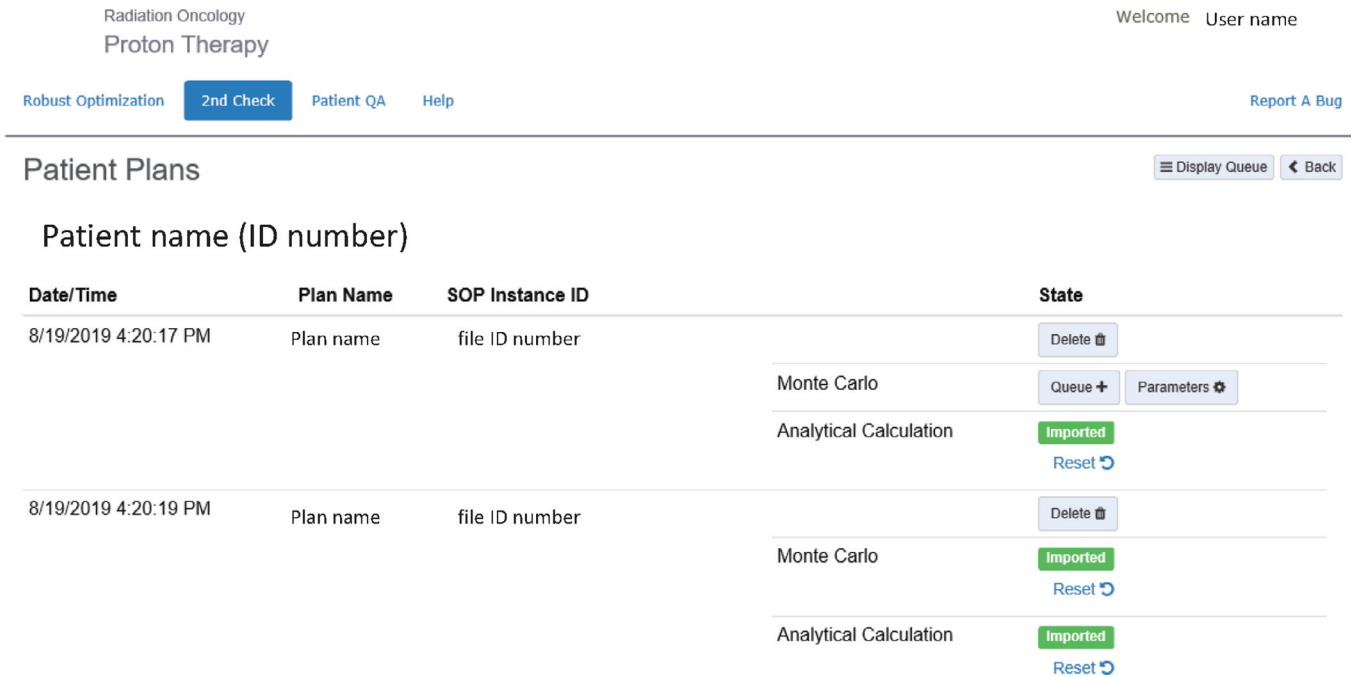


Fig. 2. User interface of the web-based platform control module. [Color figure can be viewed at wileyonlinelibrary.com]

**2.A.1. Single spot IDD curves in water**

Integrated depth dose (IDD) data for each nominal beam energy were generated using the Geant4 MC code, which has been carefully benchmarked and validated by ionization

chamber measurements.<sup>36</sup> We used the single Gaussian energy spectrum model<sup>39</sup> provided by the MCsquare manual<sup>38</sup> to fit these IDD data. The fitting parameters were mean energy, energy spread, and the number of protons per MU (P/MU) as a function of nominal beam energy. The mean energy

controlled the range, the energy spread controlled the peak to plateau ratio of the IDD curve and Bragg peak width, and the P/MU controlled the absolute dose normalization of the IDD curve. These fits were validated by comparing MCsquare-simulated IDD results with the original Geant4 IDD data.

### 2.A.2. Single spot lateral profiles in air

The proton beam optical model parameters, including spot size, spot divergence, and their correlation, were mainly controlled by fitting to in air lateral dose profiles of proton beams of all clinical energies. We used the well-benchmarked Geant4 code commissioned based on the film measurements of in-air lateral dose profiles of proton beams of all clinical energies<sup>36</sup> to generate the in-air lateral dose profiles of proton beams of all clinical energies at five depths to commission MCsquare. Field size effect measurements revealed that even an inaccuracy on the order of  $10^{-4}$  relative dose level in the lateral direction of a single spot could generate a few percent of dose inaccuracy in the center of a large field (e.g., 20 cm  $\times$  20 cm field size) due to cumulative effects of small deviations of the single spot dose lateral profiles in water.<sup>40</sup> Hence the traditional single Gaussian proton beam optic model could not give good simulation results for our proton machine and we used a second Gaussian component provided by the MCsquare beam model<sup>38</sup> to give a better fitting of the in air lateral dose profile down to  $10^{-4}$  relative dose level. This improved the accuracy of simulations with large field sizes. We validated our optical model by calculating field size factors (FSF)<sup>41</sup> for seven selected energies ranging from 71.3 to 228.8 MeV with approximate energy intervals of 20 MeV. For each energy, we tested FSF at two or three different depths with different field sizes, and compared the results with ionization chamber measurements in water.

### 2.A.3. Fine-tuning the P/MU curve based on multiple SOBPs dose measurements

Starting from the initial beam model as described above, we fine-tuned our P/MU values for certain energies based on approximately 200 spread-out Bragg peak (SOBP) central-axis point dose measurements in water measured using a PTW 34045 advanced Markus chamber (PTW, Freiburg, Germany). These measurements were carefully designed to cover a number of combinations of energy and field size at different depths. We took a total of 59 measurements for the VAC configuration, 87 measurements for the RS configuration, and 106 measurements for the ERS configuration. After fine-tuning the P/MU curve, we validated our beam model using the relative difference between simulated and measured point doses, which was calculated as (simulation – measurement)/measurement.

## 2.B. Integrating MCsquare into our web-based interface

We developed a C++-based package to (a) convert CT and plan DICOM files to text and binary input files required by

MCsquare, (b) process structure DICOM files for density override and body cropping as needed, and (c) convert MCsquare simulation results to DICOM files, which could be imported back to our commercial TPS, Eclipse<sup>TM</sup> ver. 15 (Varian Medical Systems, Palo Alto, CA), for visualization purposes. Then, in order to communicate with our TPS directly and automate the second check workflow for a busy proton clinic, we have developed some functions within MCsquare to provide the needed interface and then compiled the modified MCsquare as a library. In the C++-based software package, these functions with needed arguments would be called to integrate the MC capability into our in-house developed C++-based software. We then integrated this C++-based package to our web-based software platform, “DOSeCHECK,” which is implemented as a plugin of our TPS via Eclipse Scripting API (ESAPI). “DOSeCHECK” is an in-house developed web-based software platform.<sup>33</sup> It includes a web-based user interface, Linux-based calculation servers, and a clinical database. The architecture integrates multiple dose engines, optimizations, libraries, and communication protocols. The platform supports cross-platform usage. Figure 1 shows the workflow of using MCsquare within the DOSeCHECK software platform, and Fig. 2 shows the user interface of the web-based application control module. DOSeCHECK platform provided the needed GUI to communicate with Eclipse<sup>TM</sup> via Eclipse Scripting API (ESAPI) directly and serves as a convenient interface to use MCsquare. Both C++-based software and DOSeCHECK platform are essential components to automate the second check workflow for a busy proton clinic.

## 2.C. Validation with 12 patient geometries

To perform end-to-end tests of our new C++-based user interface and the commissioning of MCsquare, we selected 12 patient treatment plans representing typical disease sites

TABLE I. Treatment plan information for the 12 patients used in this study.

Patient	Machine type	Disease type	Number of spots [ $10^3$ ]	Body volume [ $10^3$ cm <sup>3</sup> ]	Energy range [MeV]
P1	VAC	Prostate	5.1	46.0	164–205
P2	VAC	Prostate	4.3	24.8	154–203
P3	VAC	Prostate	3.2	19.8	152–196
P4	VAC	Prostate	4.9	55.6	168–208
P5	ERS	Head and neck	4.6	14.8	130–162
P6	ERS	Head and neck	21.4	18.8	82–185
P7	ERS	Head and neck	6.4	6.8	84–203
P8	VAC	Lung	18.0	34.8	79–140
P9	VAC	Lung	25.3	44.9	77–180
P10	ERS	Brain	11.7	13.2	82–172
P11	RS	Breast	56.3	36.8	79–150
P12	RS	Craniospinal	48.3	83.0	92–198

treated at our institution (Table I). The validation was performed using two approaches: (a) comparison of simulation results with patient-specific quality assurance (PSQA) measurements<sup>34</sup> in-water, and (b) comparison to a well-benchmarked GPU-accelerated MC code<sup>10</sup> (gMC) in patient geometries. The gMC code is used clinically, but it is not an open-source code. For the details of the benchmark of the gMC code, please refer to Wan *et al.*<sup>10</sup>

### 2.C.1. Comparing with PSQA measurements in water

The PSQA procedure at our institution is to deliver treatment plans to a MatrixxPT ionization chamber array (IBA Dosimetry GmbH, Schwarzenbruck, Germany) at several depths in water. These measurements are then compared to TPS calculation results in water. For each patient field, we measured two to three axial planes with up to 1020 detection points for each plane, which provide an efficient approach and a vast amount of measurement data to validate dose engine calculations. The MCsquare simulations use 50 thousand primary protons per spot given the original CT resolution and the statistical uncertainty is around 1% or less in the target region. By setting the number of the simulated protons per spots instead of setting the total number of the simulated protons per plan, we can reach more stable statistics regardless of the field size and the number of spots. We compared our simulation results with PSQA measurements using gamma index analysis with both 3%/3 mm and 2%/2 mm criteria for each patient. Only MC voxels with relative dose greater than 10% of the maximum dose were included in the analysis<sup>42</sup> and the simulation results are used as the reference field.

Meanwhile, the two-dimensional (2D) cuts and line profiles of dose distribution between the simulation results of MCsquare and measurements were compared for each of the 12 patients. We chose three relatively complex cases to present in the following Results section, one for each treatment machine: P9 (lung) for the VAC machine, P6 (head–neck) for the ERS machine, and P12 (craniospinal) for the RS machine, respectively.

### 2.C.2. Comparing with gMC in patient geometries

In addition to validation in water, we validated our simulation results by comparing with gMC in all 12 patients. The overall accuracy validation was assessed by comparing the MCsquare results and the gMC results based on the original CT resolution using three-dimensional (3D) gamma index analysis with both the 3%/3 mm and 2%/2 mm criteria. Only voxels with relative dose greater than 10% of the maximum dose were included in the analysis.<sup>42</sup> Since the gMC code can only setup the total number of the simulated protons per plan as 100 million, in order to get a fair comparison between MCsquare and gMC, we used the same 100 million total protons per plan, instead of setting the number of the simulated

protons per spot as we did in the PSQA calculations. This setup gives about 1–2% statistical uncertainty in the target regions for most of the patients.

In addition, 2D cuts and line profiles of dose distributions generated with MCsquare and gMC were compared for the 12 patients. We chose three complex cases to present in the following results section, one for each treatment machine: P9 (lung) for the VAC machine, P6 (head–neck) for the ERS machine, and P12 (craniospinal) for the RS machine, respectively.

## 2.D. New features

Our new C++ I/O platform introduced two new important capabilities, which were not available in the Matlab-based I/O platform.

### 2.D.1. CT resampling to improve simulation efficiency

The Monte-Carlo simulation time is proportional to the total number of simulated particles, but the statistical uncertainty of simulation results is inversely proportional to the square root of the product of total number of simulated particles and the CT voxel volume (decided by the resolutions in 3D). The new I/O platform can resample the original CT using tri-linear interpolation method. For relatively uniform targets (e.g., prostate, brain, etc.), voxel volume can be increased to allow for the reduction in simulated particles and decrease the simulation time, while achieving similar statistical uncertainty. The factor of speed increase approximately equals the ratio of voxel volume between the coarser resolution and the original resolution. Here, we resampled the CTs by modifying the voxel size in all directions. In the following Results section, we will show an example comparison for a Head and Neck case with original CT resolution ( $1.27 \times 1.27 \times 2 \text{ mm}^3$ ) and the reduced resolution ( $2.5 \times 2.5 \times 2.5 \text{ mm}^3$ ). We will also show the calculation time for all 12 patients using different CT resolutions. We compared the simulation results between using the original CTs and using the resampled CTs by gamma index analysis with 2%/2 mm criteria for each patient. The simulation results from original CT resolution are used as the reference.

### 2.D.2. Biological dose calculation based on different relative biological effectiveness (RBE) models

The current practice of IMPT is to use a constant RBE value of 1.1 to convert physical doses to RBE doses.<sup>43</sup> Although there are many uncertainties in the RBE calculation, it is likely that a constant RBE value of 1.1 underestimates RBE near the end of the proton beam range and in the corresponding lateral penumbra regions<sup>43–47</sup> which may result in unexpected toxicities to the surrounding organs at risk (OARs). Although more sophisticated linear energy

transfer (LET), biological endpoint, tissue type,<sup>19,48–52</sup> track structure,<sup>53</sup> and physical dose<sup>44,54</sup> dependent proton RBE models are under development,<sup>43</sup> the recently published American Association of Physicists in Medicine Task Group Report, TG-256<sup>43</sup> suggests assessing the potential clinical consequences associated with variable RBE models and recommends LET-guided plan evaluation and LET-guided optimization in treatment planning systems (TPSs). We implemented a simplified RBE model during the postprocessing within the C++ software package using the MCsquare-generated physical dose and LET distributions. The model<sup>55</sup> we included in this work for the demonstration purpose is:

$$D_{RBE} = 1.1 \frac{\text{cGy}(RBE)}{\text{cGy}} \times D \times \left( 0.08 \frac{1}{\text{keV}/\mu\text{m}} \times LET + 0.88 \right)$$

where  $D$  is the physical dose in the unit of cGy and LET is the dose-averaged linear energy transfer in the unit of keV/ $\mu\text{m}$ . This is a simplified model, which ignores the other

factors and only considers the LET and physical dose dependence. In this model, RBE increases with LET and is 1.1 when LET = 1.5 keV/ $\mu\text{m}$ . In the following Results section, we will compare this model with the constant RBE model in case of a prostate plan.

### 3. RESULTS

#### 3.A. Single spot IDD curves in water

Figure 3 shows the commissioning results of relative IDD curves of six representative nominal beam energies. For all nominal beam energies, the average relative dose difference between the MCsquare simulation and the benchmarked Geant4 simulation in depth was within 1–2%.

#### 3.B. Single spot lateral profile in air

Figure 4 shows the FSF simulation results for three representative energies, which showed a good agreement with ionization chamber measurements (relative difference <2%).

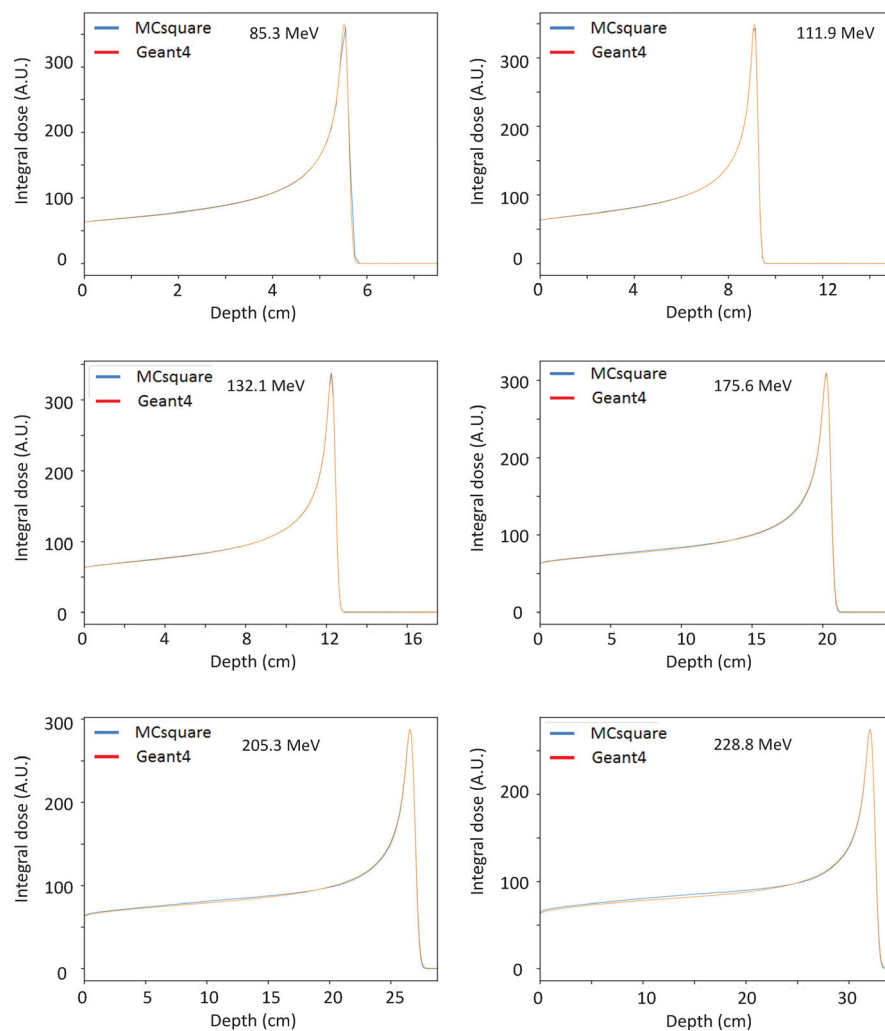


FIG. 3. Comparison of relative integrated depth dose curves of six representative energies between MCsquare and Geant4 simulation results before normalization of number of protons. The red curve corresponds to the Geant4 simulation and the blue curve corresponds to the MCsquare simulation. The comparison shows excellent agreement. [Color figure can be viewed at [wileyonlinelibrary.com](http://wileyonlinelibrary.com)]

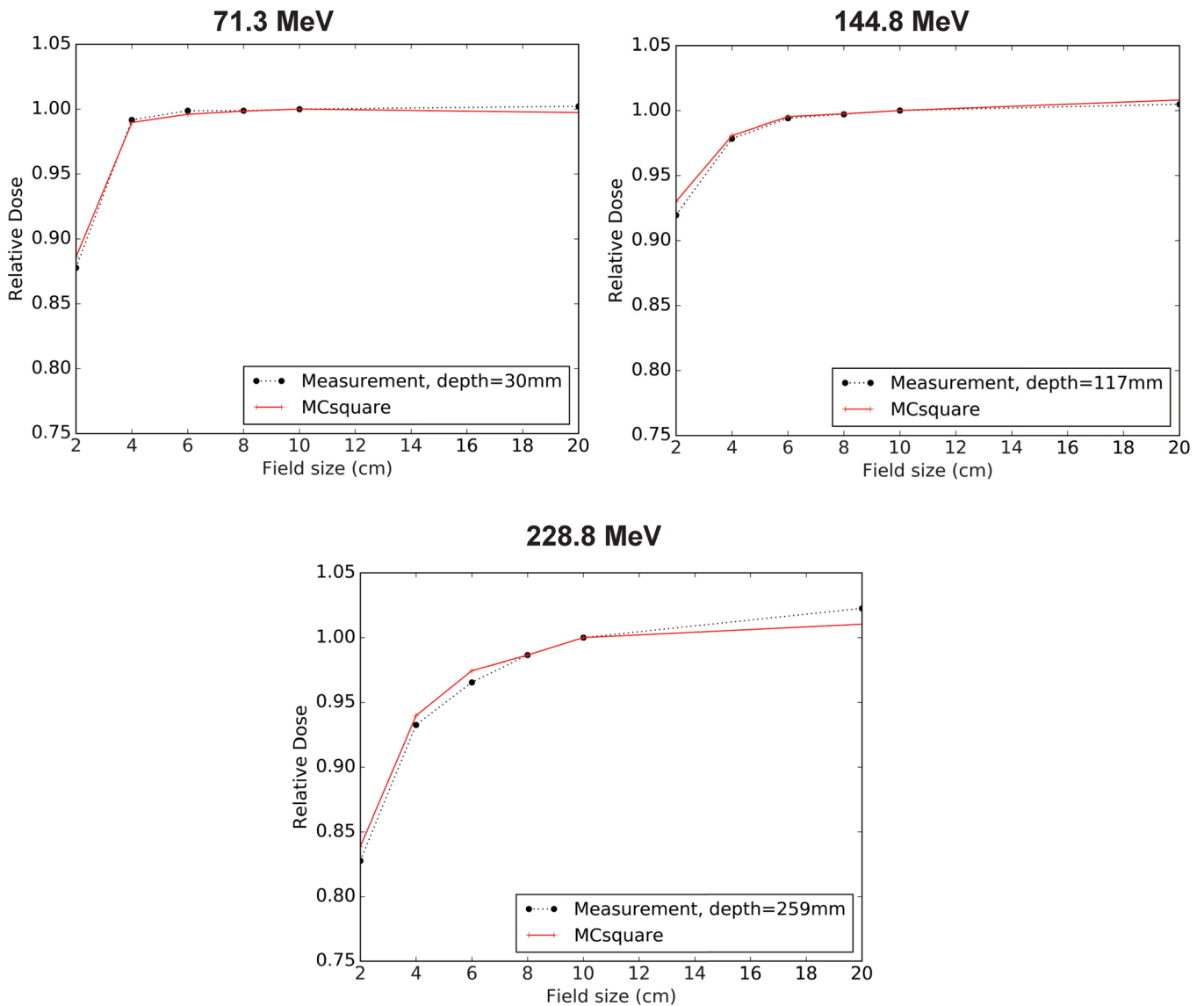


FIG. 4. Comparison of field size factor simulation results of three representative energies with different field size (from 2 cm × 2 cm to 20 cm × 20 cm) at different depths with ionization chamber measurements. Black dots are the ionization chamber measurements and the red curves correspond to our MCsquare simulation results. [Color figure can be viewed at [wileyonlinelibrary.com](http://wileyonlinelibrary.com)]

These results demonstrated that the proton beam optical model used in MCsquare can correctly model the lateral low dose tails of single spots.

### 3.C. Validation with SOBP point dose measurements

Figure 5 shows the relative differences between MCsquare simulation results and approximately 200 SOBP point dose measurements, after fine-tuning of the P/MU curve. The relative differences between MCsquare simulations and SOBP point dose measurements are within 2.5% for all cases and within 1.5% for ~85% cases. Figure 6 shows the relationship of final P/MU values vs energies and the second-order polynomial fitting for the final P/MU curve.

### 3.D. Validation in 12 patients across different disease sites

#### 3.D.1. Comparing with PSQA measurements in water

Table II summarizes the gamma analysis passing rates comparing MCsquare simulations with PSQA measurements in water using 3%/3 mm and 2%/2 mm criteria, respectively. The average gamma passing rate was 99.8% ± 0.4% using the 3%/3 mm criteria, and 99.0% ± 0.9% using the 2%/2 mm criteria. The results showed excellent agreements between MCsquare simulation and PSQA measurements in water.

Figures 7 through 9 show comparisons of 2D in-plane PSQA measurements with MCsquare calculations and gMC

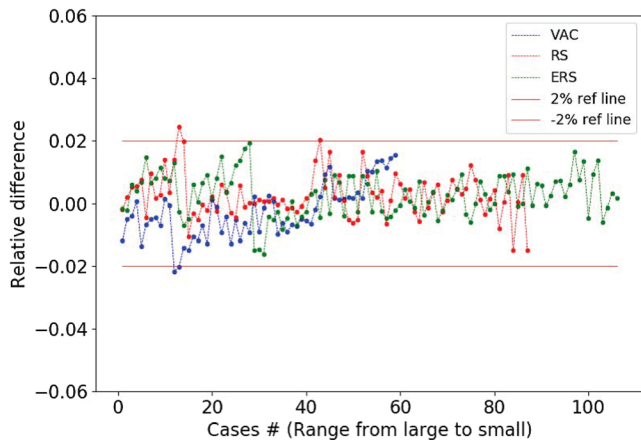


FIG. 5. Relative differences between MCsquare simulations and spread-out Bragg peak (SOBP) point dose measurements for the VAC (without range shifter), ERS (with 45 mm range shifters at 30 cm), and RS (with 45 mm range shifters at 42.5 cm) nozzle configuration, respectively. The X-axis indicates the index for different SOBP point dose measurements. [Color figure can be viewed at wileyonlinelibrary.com]

calculations for three patients (lung, head-neck, and craniospinal). We found that the MCsquare simulation results agreed well with both point dose measurements and the gMC simulation results.

**3.D.2. Comparing with gMC in 12 patients across different disease sites in patient geometries**

Table III summarizes the 3D gamma analysis passing rates of comparing MCsquare and gMC simulation results in patient geometries using both 3%/3mm and 2%/2 mm criteria, respectively. The average gamma passing rate was  $99.6\% \pm 0.2\%$  using the 3%/3 mm criteria, and  $98.0\% \pm 1.0\%$  using the 2%/2 mm criteria.

Figures 10–12 show the comparisons of dose distributions at one typical CT slice between (a) the result calculated by MCsquare and (b) the result calculated by gMC in three complex patients: P9 (lung, Fig. 10), P6 (head-neck, Fig. 11), and P12 (craniospinal, Fig. 12), respectively. The comparisons of the dose line profiles in X and Y directions calculated by MCsquare (red) and gMC (blue) as indicated with white arrows in (a) and (b) were displayed in (c) and (d), respectively. The simulation results between both MC codes agreed with each other very well.

**3.E. New features**

**3.E.1. CT resampling technique to improve the simulation efficiency**

Figure 13 shows the dose distribution difference between the results derived using two different resolutions, the original CT resolution ( $1.27\text{ mm} \times 1.27\text{ mm} \times 2\text{ mm} = 3.2\text{ mm}^3$ ) and the coarser resolution ( $2.5\text{ mm} \times 2.5\text{ mm} \times 2.5\text{ mm} = 15.6\text{ mm}^3$ ). We found that as long as CT numbers do not change sharply within the voxel size scale, the calculated dose distribution with a coarser resolution agreed well with the calculated dose distribution with a finer resolution. However, the MC simulation time was approximately five times lower with a coarser resolution compared to a finer resolution due to the 80% reduction in the number of total simulated particles. The increased speed ratio is nearly equal to the ratio of the voxel volume between two different resolutions with similar statistical uncertainty in the MCsquare simulations. Please note that this calculation time reduction ratio is estimated for the MC simulation only and the extra data pre- and postprocessing time remains almost the same when the resampled CT resolution is changed.

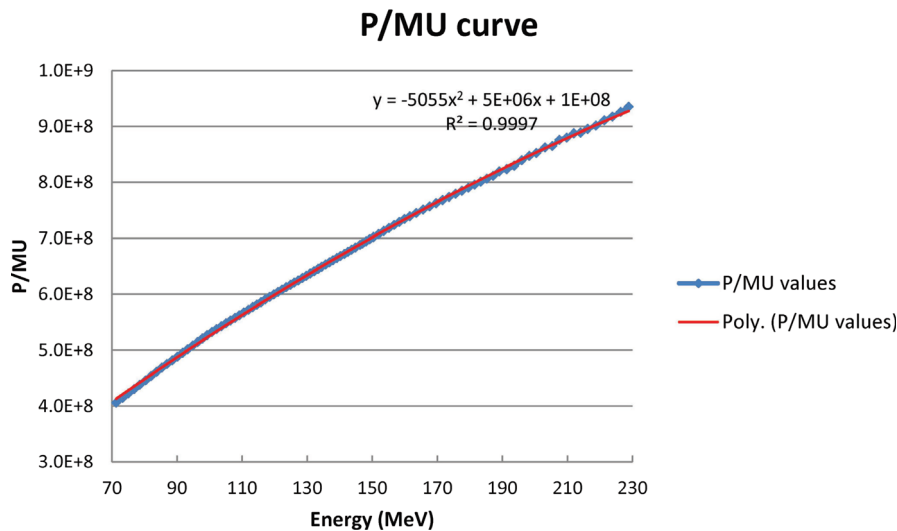


FIG. 6. Final number of protons per MU (P/MU) curve used in MCsquare. The blue dots are the final P/MU values for all energies and the red line is the second-order polynomial fitting. The curves agree well with each other. The fitting results are displayed in the figure with  $R^2 = 0.9997$ . [Color figure can be viewed at wileyonlinelibrary.com]

TABLE II. Gamma analysis passing rates comparing MCsquare simulation results with patient-specific quality assurance (PSQA) in-plane two-dimensional (2D) measurements for 12 patients across different disease sites using 3%/3 mm and 2%/2 mm criteria, respectively. A 10% relative dose threshold is used in the Gamma analysis.

Patient	Machine type	Disease type	Gamma analysis 3%/3 mm	Gamma analysis 2%/2 mm
P1	VAC	Prostate	99.7%	99.3%
P2	VAC	Prostate	99.1%	97.8%
P3	VAC	Prostate	100.0%	100.0%
P4	VAC	Prostate	99.5%	98.0%
P5	ERS	Head and neck	100.0%	99.2%
P6	ERS	Head and neck	99.0%	98.0%
P7	ERS	Head and neck	100.0%	100.0%
P8	VAC	Lung	100.0%	99.7%
P9	VAC	Lung	100.0%	99.2%
P10	ERS	Brain	100.0%	100.0%
P11	RS	Breast	100.0%	98.0%
P12	RS	Craniospinal	100.0%	98.5%
Average ± standard deviation			99.8% ± 0.4%	99.0% ± 0.9%

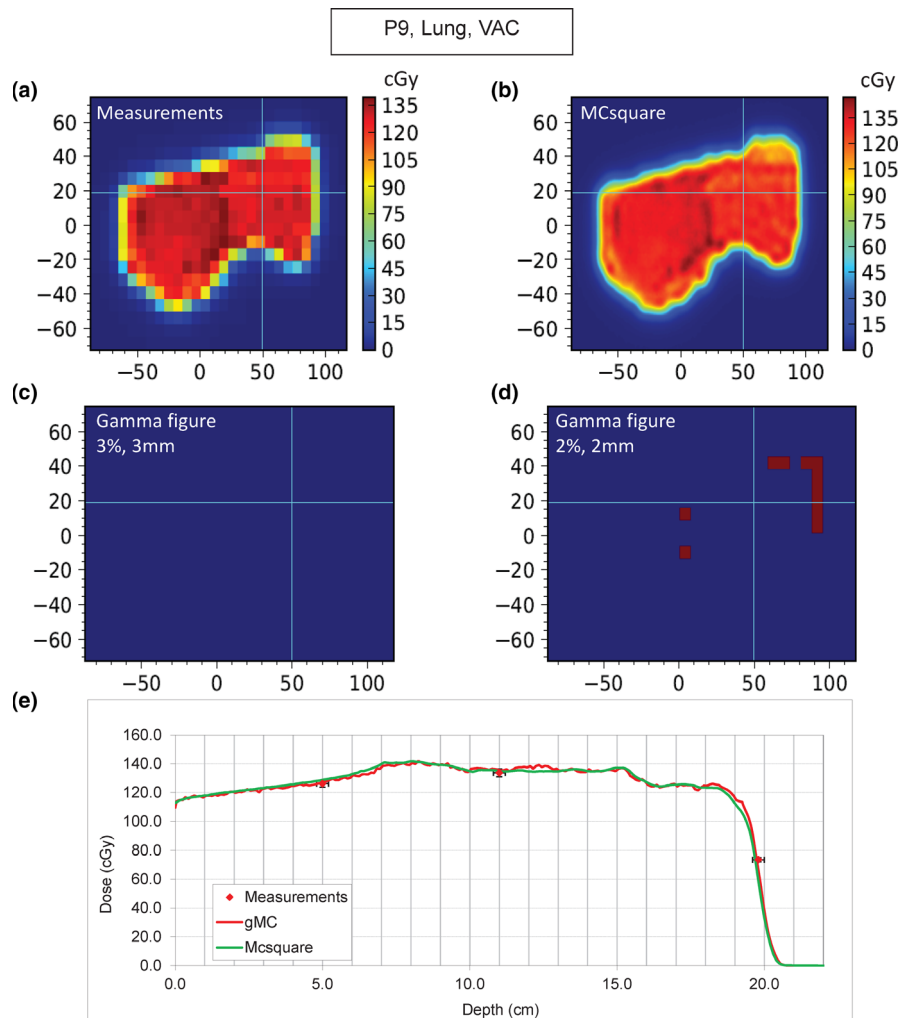


FIG. 7. Comparisons of two-dimensional in-plane patient-specific quality assurance measurements (a) vs MCsquare calculations (b) at 11 cm depth of patient P9 (lung), and the corresponding gamma analysis figures with 3%/3 mm criteria (c) and 2%/2 mm criteria (d), respectively. Panel (e) is the comparisons of dose line profiles vs depth in the beam direction through the crosshair position shown in (a) and (b), among MCsquare simulation (green), gMC simulation (red), and the matrix chamber point dose measurements with 2%/2 mm error bars at three depths (red dots). [Color figure can be viewed at wileyonlinelibrary.com]

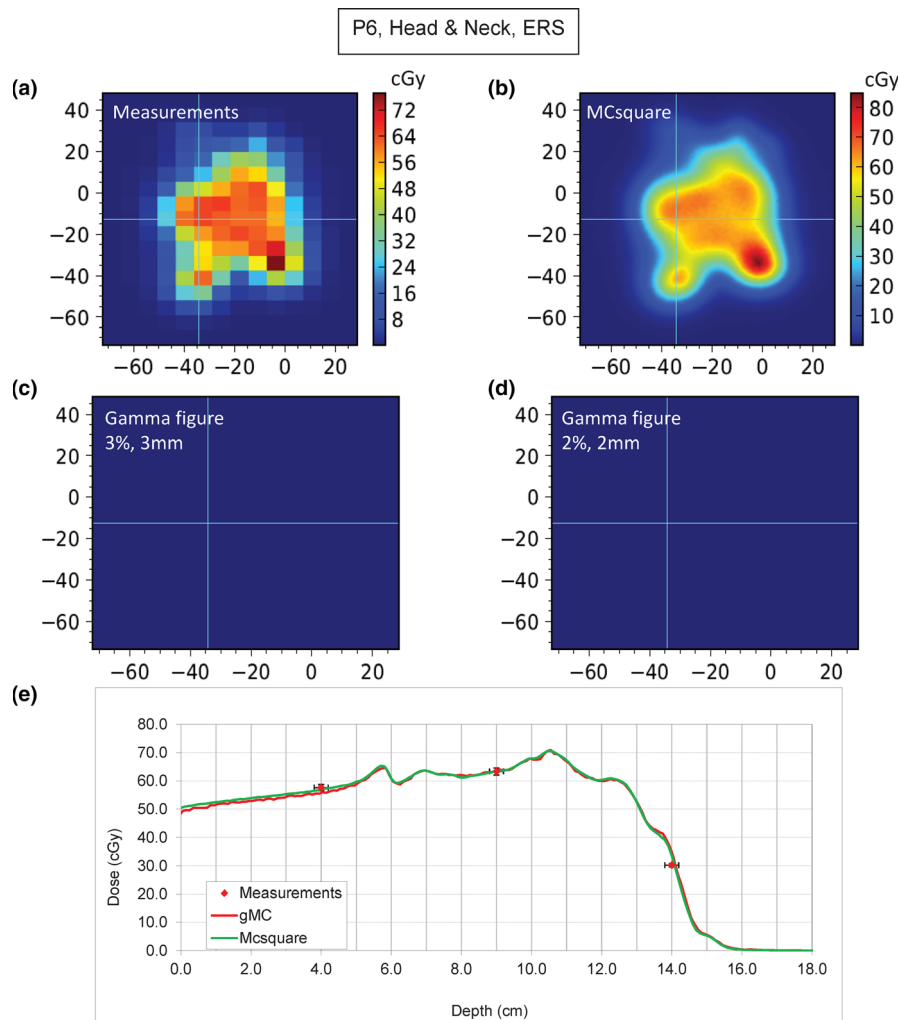


FIG. 8. Comparisons of two-dimensional in-plane patient-specific quality assurance measurements (a) vs MCsquare calculations (b) at 8 cm depth of patient P6 (head and neck), and the corresponding gamma analysis figures with 3%/3 mm criteria (c) and 2%/2 mm criteria (d), respectively. Panel (e) is the comparisons of dose line profiles vs depth in the beam direction through the crosshair position shown in (a) and (b), among MCsquare simulation (*green*), gMC simulation (*red*), and the matrix chamber point dose measurements with 2%/2 mm error bars at three depths (*red dots*). [Color figure can be viewed at [wileyonlinelibrary.com](http://wileyonlinelibrary.com)]

The MCsquare calculation time for all 12 patients using both fine CT (voxel volume =  $3.2 \text{ mm}^3$ ) and resampled CT (voxel volume =  $15.6 \text{ mm}^3$ ) is shown in Table IV. The calculation platform is dual Intel E5-2680 v3 CPU processor (24 cores).

The average simulation time was ( $6.7 \pm 4.3$ ) min for MCsquare code simulating 100 million primary protons using the fine CT voxel volume and ( $2.3 \pm 1.8$ ) min simulating 20 million primary protons using the larger CT voxel volume. Since there were extra 1–4 min for data pre- and postprocessing which remained almost the same when we varied the number of the total simulated protons, the total calculation time was not exactly five times shorter after using the coarser resampled CT resolution. The average particle tracking rate for these 12 patients is about  $(349 \pm 100) \times 10^3/\text{s}$ . The dose is only simulated in the body structure for both situations. The CT resampling markedly improved the simulation efficiency, but kept the statistical uncertainty as simulating 100 million primary protons using

the fine CT resolution. The average gamma passing rate comparing the simulation results between the original CTs and the resampled CTs using 2%/2 mm criteria is  $98.8\% \pm 1.4\%$ .

### 3.E.2. Biological dose calculation based on different RBE models

Figure 14 shows the biological dose distribution at a CT slice at isocenter calculated based on the RBE model described in the Method section. There is a significant ( $>15\%$ ) RBE dose increase in the distal edge compared with the traditional RBE = 1.1 model.

## 4. DISCUSSION

In this work, we successfully integrated the open-source MC code, MCsquare, into our C++-based I/O user interface

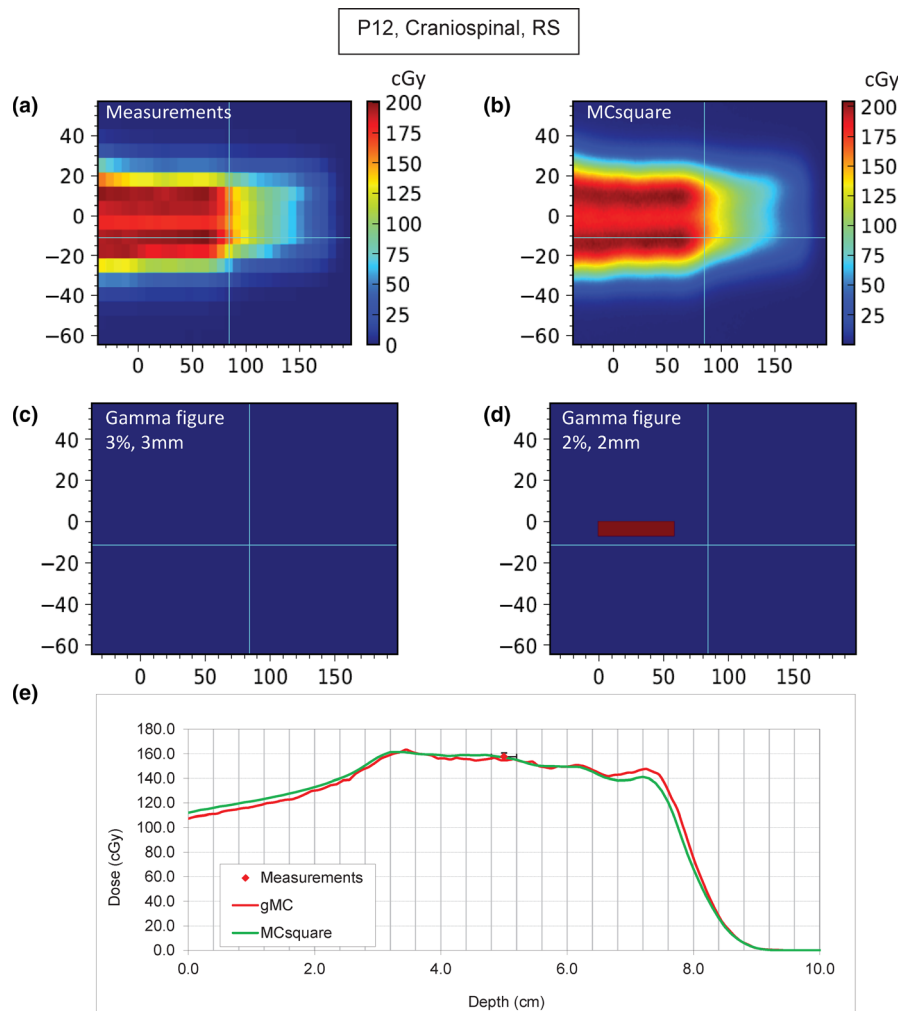


FIG. 9. Comparisons of two-dimensional in-plane patient-specific quality assurance measurements (a) vs MCsquare calculations (b) at 5 cm depth of patient P12 (craniospinal), and the corresponding gamma analysis figures with 3%/3 mm criteria (c) and 2%/2 mm criteria (d), respectively. Panel (e) is the comparisons of dose line profiles vs depth in the beam direction through the crosshair position shown in (a) and (b), among MCsquare simulation (green), gMC simulation (red), and the matrix chamber point dose measurements with 2%/2 mm error bars at one depth (red dot). [Color figure can be viewed at [wileyonlinelibrary.com](http://wileyonlinelibrary.com)]

and our web-based software platform with MPI calculation capability to replace the original Matlab-based I/O platform, which rendered it capable of communicating with our commercial TPS directly and convenient for routine clinical use. Users with no MATLAB or C/C++ programming experience were able to use it with little to no assistance. We also improved calculation efficiency by adopting a variable resolution technique and expanded MCsquare's capability by adding a model-based biological dose calculation function for biological plan dose evaluation in IMPT. After careful and comprehensive commissioning, MCsquare simulations showed very good agreement with measurements and the well-benchmarked GPU-accelerated MC code. This is the first time that the accuracy of open source MCsquare is validated for a synchrotron-based proton system.

For the single spot IDD validation, we observed a discrepancy near the Bragg peak for relatively low energy spots. This deviation is mainly due to the voxel size used in the scoring of the MC simulation results and not an inaccuracy of the

MCsquare algorithms. Although the Geant4 simulation results used for the commissioning purpose were performed with 0.1 mm resolution in depth, our MCsquare simulation results, in order to match the clinical CT resolution better, were performed using 1 mm resolution in depth. For low energy IDD curves, the typical widths of the Bragg peaks are close to or even smaller in width than 1 mm, which results in this deviation.

We used the well-benchmarked Geant4 code commissioned based on the film measurements of in-air lateral dose profiles of proton beams of all clinical energies<sup>36</sup> to generate the in-air lateral dose profiles of proton beams of all clinical energies at five depths to generate the parameters of beam optical model, including spot size, spot divergence, and their correlation. Then, we validated the spot's in-air lateral profile parameters after commissioning using the more clinically relevant FSF tests in water. The FSF tests validated the cumulative effects of the small deviations of the single spot dose lateral profiles in water down to  $10^{-4}$  relative lateral dose level. Our results

TABLE III. Three-dimensional Gamma analysis passing rates of comparing MCsquare and gMC simulation results for 12 patients across different disease sites using 3%/3 mm and 2%/2 mm criteria, respectively. A 10% relative dose threshold is used in the Gamma analysis in Column 4 and 5.

Patient	Machine type	Disease type	Gamma analysis 3%/3 mm	Gamma analysis 2%/2 mm
P1	VAC	Prostate	99.7%	97.0%
P2	VAC	Prostate	99.7%	98.7%
P3	VAC	Prostate	99.7%	98.3%
P4	VAC	Prostate	99.5%	96.5%
P5	ERS	Head and neck	99.8%	98.8%
P6	ERS	Head and neck	99.5%	97.0%
P7	ERS	Head and neck	99.8%	99.3%
P8	VAC	Lung	99.7%	98.8%
P9	VAC	Lung	99.1%	99.4%
P10	ERS	Brain	99.7%	98.2%
P11	RS	Breast	99.8%	98.0%
P12	RS	Craniospinal	99.5%	96.5%
Average ± standard deviation			99.6% ± 0.2%	98.0% ± 1.0%

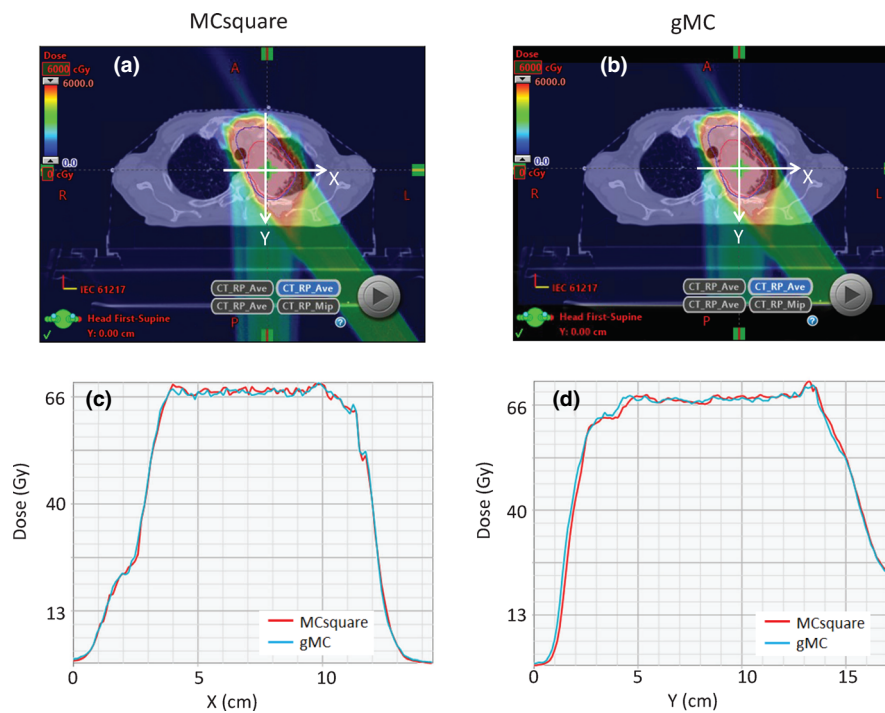


FIG. 10. Comparisons of the dose distributions at one typical computed tomography slice between (a) the result calculated using MCsquare and (b) the result calculated using gMC in patient P9 (lung). The comparisons of the dose line profiles in X and Y directions calculated using MCsquare (red) and gMC (blue) as indicated by white arrows in (a) and (b) were displayed in (c) and (d), respectively. [Color figure can be viewed at wileyonlinelibrary.com]

showed a good agreement between MCsquare simulations and measurements in most of the situations.

After using the CT resampling and body cropping approach, the calculation time for CPU-based MCsquare was (2.3 ± 1.8) min, which made MCsquare an efficient solution as a dose calculation engine for routine clinical second dose check and MC-based robust optimization in IMPT. Here, we resampled the CTs by modifying the resolution in all directions and the difference of the simulation results between using the original CTs and using the resampled CTs was

found to be clinically insignificant for the 12 patients included in this study. The average gamma passing rate using 2%/2 mm criteria is 98.8% ± 1.4%. Here, we did not study the optimal threshold of CT resampling to balance the calculation accuracy and time based on different CT number gradients. In the future, people can enhance this CT resampling method by introducing more advanced methods like adaptive resolution method to further improve the calculation speed.

In this paper, we start from a simplified RBE model which only considers the LET and physical dose dependence as a

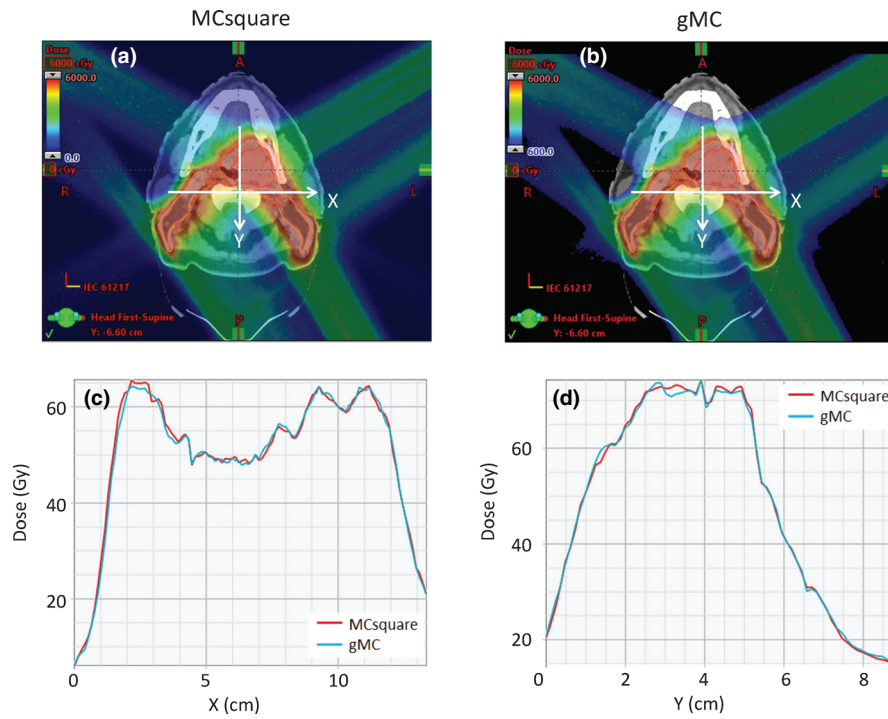


FIG. 11. Comparisons of the dose distributions at one typical computed tomography slice between (a) the result calculated using MCsquare and (b) the result calculated using gMC in patient P6 (head and neck). The comparisons of the dose line profiles in X and Y directions calculated using MCsquare (red) and gMC (blue) as indicated by white arrows in (a) and (b) were displayed in (c) and (d), respectively. [Color figure can be viewed at wileyonlinelibrary.com]

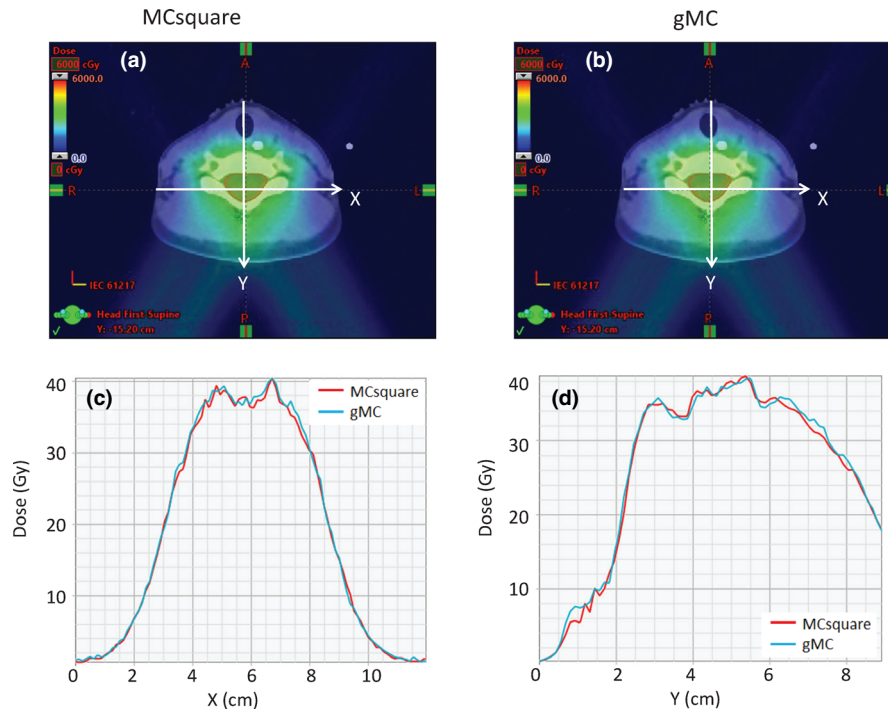


FIG. 12. Comparisons of the dose distributions at one typical computed tomography slice between (a) the result calculated by MCsquare and (b) the result calculated using gMC in patient P12 (craniospinal). The comparisons of the dose line profiles in X and Y directions calculated using MCsquare (red) and gMC (blue) as indicated by white arrows in (a) and (b) were displayed in (c) and (d), respectively. [Color figure can be viewed at wileyonlinelibrary.com]

demonstration. In the future we may implement other, more sophisticated, RBE models within our software platform. Considering the high calculation efficiency and accuracy of

our web-based software platform, we can perform the correlation study of patient outcomes with the RBE doses calculated using a variety of RBE models. In the future we may be able

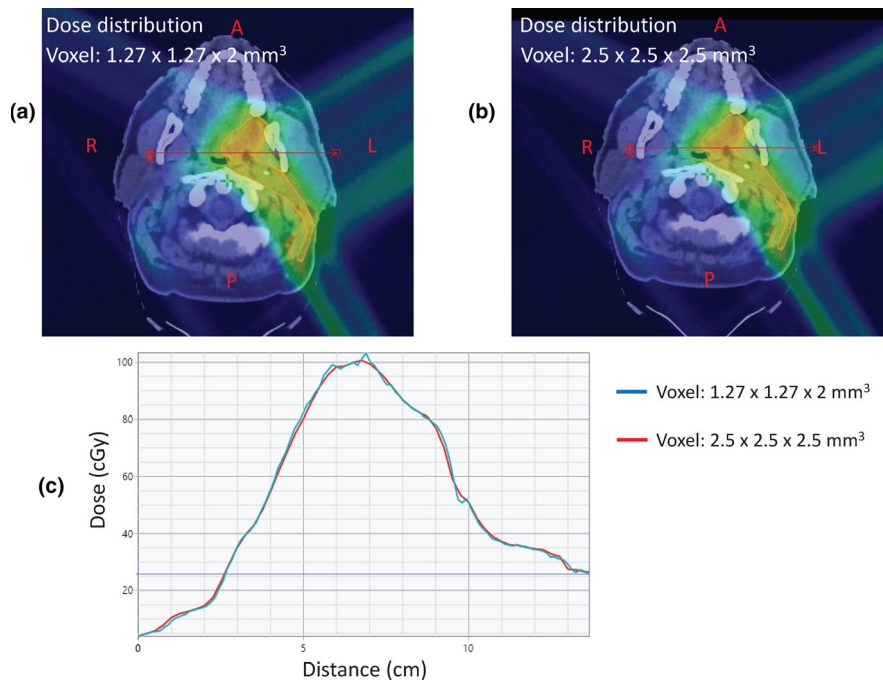


FIG. 13. Comparison of dose distributions using (a) the original computed tomography (CT) (voxel size 1.27 mm × 1.27 mm × 2 mm) and (b) the resampled CT (voxel size 2.5 mm × 2.5 mm × 2.5 mm) in patient P6 (head and neck). Panels (a) and (b) show the same CT slice at the tumor location. Panel (c) shows the comparison of the dose line profile indicated by red arrows in Panel (a) and (b). The blue curve corresponds to the result with the original CT and the red curve corresponds to the result with the resampled CT. The two dose line profiles show excellent agreement. [Color figure can be viewed at wileyonlinelibrary.com]

TABLE IV. Comparison of MCsquare calculation time between using the original computed tomography (CT) and the resampled CT.

Patient	Machine type	Disease type	Calculation time (min), original CT	Calculation time (min), resampled CT	Gamma analysis 2%/2 mm	Tracking rate (× 10 <sup>3</sup> /s)
P1	VAC	Prostate	4.4	1.2	99.9%	417
P2	VAC	Prostate	3.9	1.0	99.7%	455
P3	VAC	Prostate	3.7	1.0	99.8%	476
P4	VAC	Prostate	4.8	1.3	99.7%	377
P5	ERS	Head and neck	4.0	1.0	99.4%	435
P6	ERS	Head and neck	6.5	2.1	98.9%	286
P7	ERS	Head and neck	6.9	2.7	99.9%	370
P8	VAC	Lung	6.5	2.0	98.8%	294
P9	VAC	Lung	6.6	2.1	95.4%	298
P10	ERS	Brain	6.5	2.3	99.4%	307
P11	RS	Breast	6.8	3.3	97.8%	370
P12	RS	Craniospinal	19.5	7.5	97.1%	107
Average ± standard deviation			6.7 ± 4.3	2.3 ± 1.8	98.8% ± 1.4%	349 ± 100

The MCsquare calculation time of simulating 100 million primary protons for all 12 patients using the CT voxel volume (3.2 mm<sup>3</sup>) similar as the usual raw CT voxel volume (e.g., 1.25 mm × 1.25 mm × 2 mm) used in our center (Column 4) and the MCsquare calculation time of simulating 20 million primary protons for all 12 patients using resampled CT (voxel volume 2.5 mm × 2.5 mm × 2.5 mm = 15.6 mm<sup>3</sup>) (Column 5). The dose is only simulated in the body structure for both situations. The calculation platform is dual Intel E5-2680 v3 CPU processor (24 cores with 2 threads per core). The Gamma analysis passing rates comparing the simulation results between the original CT resolution and the resampled CT resolution using 2%/2 mm criteria are shown in Column 6. The primary proton tracking rates are shown in Column 7.

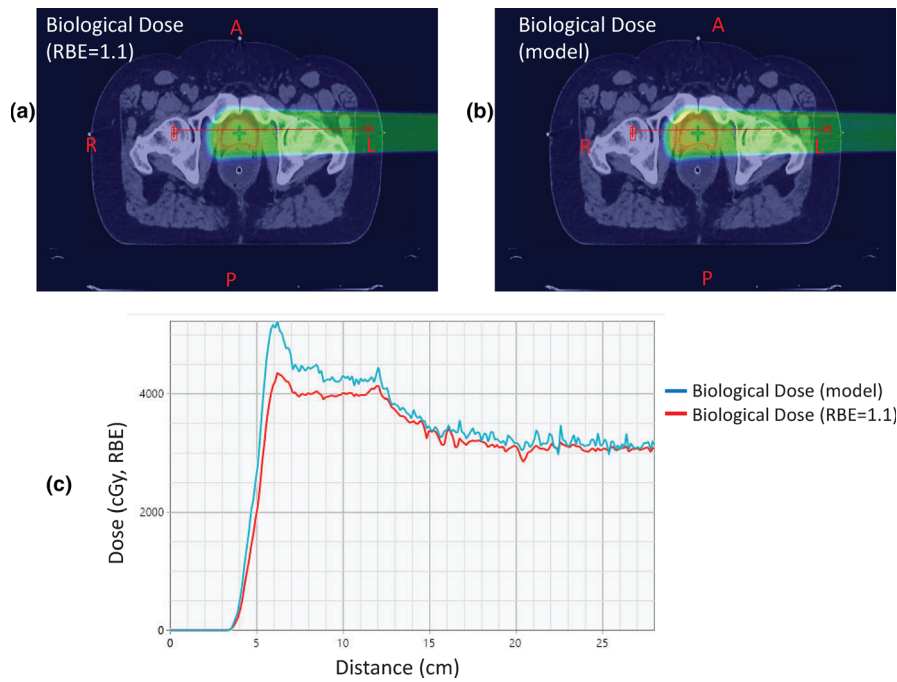


FIG. 14. Comparison of biological dose distributions based on two different relative biological equivalent (RBE) models in patient P1 (prostate): (a) fixed RBE = 1.1 and (b) LET-dependent variable RBE. Panel (c) shows the comparison of the biological dose line profiles indicated by red arrows in Panel (a) and (b) between the two biological dose calculations. [Color figure can be viewed at [wileyonlinelibrary.com](http://wileyonlinelibrary.com)]

to find improved RBE models that fit the patient outcomes better. This will be the topic of future study.

In the future, we will integrate MCsquare dose engine into our existing robust optimization software to achieve MC-based robust optimization. The more accurate dose and LET calculation from MCsquare can achieve better results for LET-guided robust optimization,<sup>54,56,57</sup> especially in inhomogeneous disease sites like lung and head and neck cancer treated by IMPT.

## 5. CONCLUSIONS

MCsquare was successfully commissioned for a synchrotron-based proton delivery system and integrated into our C++-based I/O user interface and our web-based software platform. We also improved the calculation efficiency by implementing a variable resolution technique and expanded its capability by adding a simple model-based biological dose calculation. The dose distributions calculated using MCsquare agreed well with measurements in water and gMC calculations in patient geometries. MCsquare is sufficiently fast to be used as a clinical second check dose engine. In the future, we plan to integrate MCsquare into our robust optimization software to achieve MC-based and LET-guided robust optimization in IMPT and use it as a fast and convenient computation platform to investigate which is the most appropriate RBE model in IMPT to predict patient outcome.

## ACKNOWLEDGMENTS

This research was supported by the Arizona Biomedical Research Commission Investigator Award (ADHS16-162521), The Lawrence W. and Marilyn W. Matteson Fund for Cancer Research, and the Kemper Marley Foundation.

## CONFLICT OF INTEREST

The authors have no conflict to disclose.

<sup>a)</sup>Authors to whom correspondence should be addressed. Electronic mails: [liu.wei@mayo.edu](mailto:liu.wei@mayo.edu), [shen.jiajian@Mayo.edu](mailto:shen.jiajian@Mayo.edu).

## REFERENCES

1. Agostinelli S, Allison J, Ka A, et al. GEANT4—a simulation toolkit. *Nucl Instrum Methods Phys Res A*. 2003;506:250–303.
2. Waters L, Hendricks J, McKinney G. *Monte Carlo N-particle transport code system for multiparticle and high energy applications*. Los Alamos, NM: Los Alamos National Laboratory; 2002.
3. Battistoni G, Broggi F, Brugger M, et al. The FLUKA code and its use in hadron therapy. *Nuovo Cimento Soc Ital Fis C*. 2008;31:69–75.
4. Kozłowska WS, Böhlen TT, Cuccagna C, et al. FLUKA particle therapy tool for Monte Carlo independent calculation of scanned proton and carbon ion beam therapy. *Phys Med Biol*. 2019;64:075012.
5. Perl J, Shin J, Schümann J, Faddegon B, Paganetti H. TOPAS: an innovative proton Monte Carlo platform for research and clinical applications. *Med Phys*. 2012;39:6818–6837.

6. Hong L, Goitein M, Bucciolini M, et al. A pencil beam algorithm for proton dose calculations. *Phys Med Biol*. 1996;41:1305–1330.
7. Schaffner B, Pedroni E, Lomax A. Dose calculation models for proton treatment planning using a dynamic beam delivery system: an attempt to include density heterogeneity effects in the analytical dose calculation. *Phys Med Biol*. 1999;44:27–41.
8. Younkin JE, Morales DH, Shen J, et al. Clinical validation of a ray-casting analytical dose engine for spot scanning proton delivery systems. *Technol Cancer Res Treatm*. 2019;18:1533033819887182.
9. Taylor PA, Kry SF, Followill DS. Pencil beam algorithms are unsuitable for proton dose calculations in lung. *Int J Radiat Oncol Biol Phys*. 2017;99:750–756.
10. Wan Chan Tseung H, Ma J, Beltran C. A fast GPU-based Monte Carlo simulation of proton transport with detailed modeling of nonelastic interactions. *Med Phys*. 2015;42:2967–2978.
11. Jia X, Schümann J, Paganetti H, Jiang SB. GPU-based fast Monte Carlo dose calculation for proton therapy. *Phys Med Biol*. 2012;57:7783–7797.
12. Schiavi A, Senzacqua M, Pioli S, et al. Fred: a GPU-accelerated fast-Monte Carlo code for rapid treatment plan recalculation in ion beam therapy. *Phys Med Biol*. 2017;62:7482–7504.
13. Souris K, Lee JA, Sterpin E. Fast multipurpose Monte Carlo simulation for proton therapy using multi-and many-core CPU architectures. *Med Phys*. 2016;43:1700–1712.
14. Saini J, Maes D, Egan A, et al. Dosimetric evaluation of a commercial proton spot scanning Monte-Carlo dose algorithm: comparisons against measurements and simulations. *Phys Med Biol*. 2017;62:7659–7681.
15. Lin L, Huang S, Kang M, et al. A benchmarking method to evaluate the accuracy of a commercial proton monte carlo pencil beam scanning treatment planning system. *J Appl Clin Med Phys*. 2017;18:44–49.
16. Chih-Wei Chang SH, Harms J, Zhou J, et al. A standardized commissioning framework of Monte Carlo dose calculation algorithms for proton pencil beam scanning treatment planning systems. Conditionally accepted by Medical Physics.
17. Ma J, Wan Chan Tseung HS, Herman MG, Beltran C. A robust intensity modulated proton therapy optimizer based on Monte Carlo dose calculation. *Med Phys*. 2018;45:4045–4054.
18. Gu W, Ruan D, O'Connor D, et al. Robust optimization for intensity-modulated proton therapy with soft spot sensitivity regularization. *Med Phys*. 2019;46:1408–1425.
19. An Y, Shan J, Patel SH, et al. Robust intensity-modulated proton therapy to reduce high linear energy transfer in organs at risk. *Med Phys*. 2017;44:6138–6147.
20. Unkelbach J, Bortfeld T, Martin BC, Soukup M. Reducing the sensitivity of IMPT treatment plans to setup errors and range uncertainties via probabilistic treatment planning. *Med Phys*. 2009;36:149–163.
21. Unkelbach J, Chan TC, Bortfeld T. Accounting for range uncertainties in the optimization of intensity modulated proton therapy. *Phys Med Biol*. 2007;52:2755–2773.
22. Pflugfelder D, Wilkens J, Oelfke U. Worst case optimization: a method to account for uncertainties in the optimization of intensity modulated proton therapy. *Phys Med Biol*. 2008;53:1689–1700.
23. Fredriksson A, Forsgren A, Hårdemark B. Minimax optimization for handling range and setup uncertainties in proton therapy. *Med Phys*. 2011;38:1672–1684.
24. Fredriksson A. A characterization of robust radiation therapy treatment planning methods—from expected value to worst case optimization. *Med Phys*. 2012;39:5169–5181.
25. Wei L, Yupeng L, Xiaoqiang L, Wenhua C, Xiaodong Z. Influence of robust optimization in intensity-modulated proton therapy with different dose delivery techniques. *Med Phys*. 2012;39:3089–3101.
26. Liu W, Frank SJ, Li X, et al. Effectiveness of robust optimization in intensity-modulated proton therapy planning for head and neck cancers. *Med Phys*. 2013;40:051711.
27. Liu W, Liao Z, Schild SE, et al. Impact of respiratory motion on worst-case scenario optimized intensity modulated proton therapy for lung cancers. *Pract Radiat Oncol*. 2015;5:e77–e86.
28. An Y, Liang J, Schild SE, Bues M, Liu W. Robust treatment planning with conditional value at risk chance constraints in intensity-modulated proton therapy. *Med Phys*. 2017;44:28–36.
29. Buti G, Souris K, Montero AMB, Lee JA, Sterpin E. Towards fast and robust 4D optimization for moving tumors with scanned proton therapy. *Med Phys*. 2019;46:5434–5443.
30. Souris K, Montero AB, Janssens G, Di Perri D, Sterpin E, Lee JA. Monte Carlo methods to comprehensively evaluate the robustness of 4D treatments in proton therapy. *Med Phys*. 2019;46:4676–4684.
31. Huang S, Kang M, Souris K, et al. Validation and clinical implementation of an accurate Monte Carlo code for pencil beam scanning proton therapy. *J Appl Clin Med Phys*. 2018;19:558–572.
32. Huang S, Souris K, Li S, et al. Validation and application of a fast Monte Carlo algorithm for assessing the clinical impact of approximations in analytical dose calculations for pencil beam scanning proton therapy. *Med Phys*. 2018;45:5631–5642.
33. Augustine KE, Walsh TJ, Beltran CJ, et al. Spot scanning proton therapy plan assessment: design and development of a dose verification application for use in routine clinical practice. Paper presented at: Medical Imaging 2016: Physics of Medical Imaging; 2016.
34. Hernandez Morales D, Shan J, Liu W, et al. Automation of routine elements for spot-scanning proton patient-specific quality assurance. *Med Phys*. 2019;46:5–14.
35. Shen J, Tryggestad E, Younkin JE, et al. Using experimentally determined proton spot scanning timing parameters to accurately model beam delivery time. *Med Phys*. 2017;44:5081–5088.
36. Ding X, Liu W, Shen J, et al. Use of a radial projection to reduce the statistical uncertainty of spot lateral profiles generated by Monte Carlo simulation. *J Appl Clin Med Phys*. 2017;18:88–96.
37. Anand A, Sahoo N, Zhu XR, et al. A procedure to determine the planar integral spot dose values of proton pencil beam spots. *Med Phys*. 2012;39:891–900.
38. Commissioning procedure for MCsquare. [http://www.openmcsquare.org/documentation\\_commissioning.html](http://www.openmcsquare.org/documentation_commissioning.html)
39. Grevillot L, Bertrand D, Dessy F, Freud N, Sarrut D. A Monte Carlo pencil beam scanning model for proton treatment plan simulation using GATE/GEANT4. *Phys Med Biol*. 2011;56:5203–5219.
40. Pedroni E, Scheib S, Böhringer T, et al. Experimental characterization and physical modelling of the dose distribution of scanned proton pencil beams. *Phys Med Biol*. 2005;50:541.
41. Shen J, Lentz JM, Hu Y, et al. Using field size factors to characterize the in-air fluence of a proton machine with a range shifter. *Radiat Oncol*. 2017;12:52.
42. Miften M, Olch A, Mihailidis D, et al. Tolerance limits and methodologies for IMRT measurement-based verification QA: recommendations of AAPM Task Group No. 218. *Med Phys*. 2018;45:e53–e83.
43. Paganetti H, Blakely E, Carabe-Fernandez A, et al. Report of the AAPM TG-256 on the relative biological effectiveness of proton beams in radiation therapy. *Med Phys*. 2019;46:e53–e78.
44. Paganetti H. Relative biological effectiveness (RBE) values for proton beam therapy. Variations as a function of biological endpoint, dose, and linear energy transfer. *Phys Med Biol*. 2014;59:R419–R472.
45. Gentile MS, Yeap BY, Paganetti H, et al. Brainstem injury in pediatric patients with posterior fossa tumors treated with proton beam therapy and associated dosimetric factors. *Int J Radiat Oncol Biol Phys*. 2018;100:719–729.
46. Underwood TS, Grassberger C, Bass R, et al. Asymptomatic Late-phase radiographic changes among chest-wall patients are associated with a proton RBE exceeding 1.1. *Int J Radiat Oncol Biol Phys*. 2018;101:809–819.
47. Peeler CR, Mirkovic D, Titt U, et al. Clinical evidence of variable proton biological effectiveness in pediatric patients treated for ependymoma. *Radiation Oncol*. 2016;121:395–401.
48. Wilkens J, Oelfke U. A phenomenological model for the relative biological effectiveness in therapeutic proton beams. *Phys Med Biol*. 2004;49:2811–2825.
49. Carabe A, Moteabbed M, Depauw N, Schuemann J, Paganetti H. Range uncertainty in proton therapy due to variable biological effectiveness. *Phys Med Biol*. 2012;57:1159–1172.
50. Wedenberg M, Lind BK, Hårdemark B. A model for the relative biological effectiveness of protons: the tissue specific parameter  $\alpha/\beta$  of photons is a predictor for the sensitivity to LET changes. *Acta Oncol*. 2013;52:580–588.

51. McNamara AL, Schuemann J, Paganetti H. A phenomenological relative biological effectiveness (RBE) model for proton therapy based on all published in vitro cell survival data. *Phys Med Biol*. 2015;60:8399.
52. Grün R, Friedrich T, Krämer M, Scholz M. Systematics of relative biological effectiveness measurements for proton radiation along the spread out Bragg peak: experimental validation of the local effect model. *Phys Med Biol*. 2017;62:890–908.
53. Paganetti H, Goitein M. Biophysical modelling of proton radiation effects based on amorphous track models. *Int J Radiat Biol*. 2001;77:911–928.
54. Unkelbach J, Botas P, Giantsoudi D, Gorissen BL, Paganetti H. Reoptimization of intensity modulated proton therapy plans based on linear energy transfer. *Int J Radiat Oncol Biol Phys*. 2016;96:1097–1106.
55. Beltran C, Tseung HWC, Augustine KE, et al. Clinical implementation of a proton dose verification system utilizing a GPU accelerated Monte Carlo engine. *Int J Part Ther*. 2016;3:312–319.
56. Giantsoudi D, Grassberger C, Craft D, Niemierko A, Trofimov A, Paganetti H. Linear energy transfer-guided optimization in intensity modulated proton therapy: feasibility study and clinical potential. *Int J Radiat Oncol Biol Phys*. 2013;87:216–222.
57. Ödén J, Eriksson K, Toma-Dasu I. Inclusion of a variable RBE into proton and photon plan comparison for various fractionation schedules in prostate radiation therapy. *Med Phys*. 2017;44:810–822.